

Dynamics of hadron strong production and decay

T. J. Burns*, F. E. Close† and C. E. Thomas‡

*Rudolf Peierls Centre for Theoretical Physics, University of Oxford,
1 Keble Rd., Oxford, OX1 3NP, United Kingdom*

(Dated: September 12, 2007)

We generalize results of lattice QCD to determine the spin-dependent symmetries and factorization properties of meson production in OZI allowed processes. This explains some conjectures previously made in the literature about axial meson decays and gives predictions for exclusive decays of vector charmonia, including ways of establishing the structure of $Y(4260)$ and $Y(4325)$ from their S-wave decays. Factorization gives a selection rule which forbids $e^+e^- \rightarrow D^*D_2$ near threshold with the tensor meson in helicity 2. A different pattern of amplitudes is expected for heavy flavour production such as $e^+e^- \rightarrow \psi + \chi_j$ than for their charmed or light flavoured counterparts.

I. INTRODUCTION

The dynamics of strong decay amplitudes are poorly understood. Definitive answers are not known to questions as basic as: (i) are the $q\bar{q}$ created in an OZI allowed decay spin singlet or spin triplet; (ii) what is their overall J^{PC} ; (iii) are the $q\bar{q}$ created from the energy of the strong confinement field, or from a hard gluon? It is our purpose in this paper to address these questions. We shall show that results from lattice QCD imply that light $q\bar{q}$ are produced in spin triplet with an effective factorization of constituent spin and orbital degrees of freedom such that the $q\bar{q}$ in the initial meson are passive spectators. By contrast, if heavy flavours are created, as in $e^+e^- \rightarrow \psi + \chi_J$, factorization is broken with spin and momentum transferred from the initial $c\bar{c}$ to the created pair, such as by a hard gluon. This implies a radically different spin dependence of amplitudes, and of angular distributions, in analogue processes such as $e^+e^- \rightarrow \omega f_2$ relative to $e^+e^- \rightarrow \psi \chi_2$.

While Lattice QCD is now a mature guide for the masses of glueballs and hybrids, at least in the quenched approximation [1, 2], it is not yet mature enough to determine hadronic decays extensively. Consequently, at a fundamental level the dynamics of such decays is not yet established. Flux tube models of both spectra [3, 4] and decays [5, 6] have been developed, in part stimulated by attempts to model the lattice, and lattice work has confirmed their spectroscopy [2, 4]. The lattice is now beginning to confirm aspects of the flux tube model for some decays: specifically the lattice QCD studies of the decays of hybrid $1^{-+} \rightarrow \pi b_1$ and πf_1 [7] show quantitative features that were anticipated in flux-tube models [5, 6], and in ref [8] we showed that these approaches exhibit remarkable agreement when compared under the same kinematic conditions. Specifically, for S-wave decay amplitudes at zero-recoil the results are consistent with

$$a(\pi_1 \rightarrow \pi + b_1[1P_1]) = 2a(\pi_1 \rightarrow \pi + f_1[3P_1]). \quad (1)$$

where π_1 denotes the first gluonic excited hybrid with $J^{PC} = 1^{-+}$.

In section II we describe the underlying assumptions of the factorization hypothesis: (i) the hadrons' spins, j , separate into two parts - the intrinsic spins of the constituents s and a residual component that transforms as angular momentum l , (ii) the l and s degrees of freedom act independently throughout the transition ("factorization"), (iii) the $q\bar{q}$ created in the decay are coupled to spin-triplet. In section IIA we demonstrate that the above ratio is immediate within the factorization hypothesis. We identify further implications of factorization for the decays of axial and vector mesons in sections IIB and IIC; the former confirms and explains a conjecture of [9] and the latter has implications for charmed meson production from a $\psi(^3S_1)$ initial state. A helicity selection rule is derived implying that in $e^+e^- \rightarrow D^*D_2$ near threshold or from a $\psi(^3S_1)$ initial state the D_2 cannot be produced with helicity two. In section IID we apply the results of factorization to the decays of $c\bar{c}$ to charmed mesons near threshold in relative S-waves, and identify ways to distinguish between hybrid and conventional interpretations of enigmatic ψ -like states such as $Y(4260)$ or $Y(4325)$.

* e-mail: burns@thphys.ox.ac.uk

† e-mail: F.Close1@physics.ox.ac.uk

‡ e-mail: C.Thomas1@physics.ox.ac.uk

In section III we discuss application to e^+e^- annihilation for light and heavy flavours. We show that decays triggered by hard gluons violate factorization, and that emerging data on $e^+e^- \rightarrow \psi + \chi_j$ appear to support this. We propose tests for factorization and hard gluon production mechanisms in $e^+e^- \rightarrow \psi + \chi_j$ near threshold.

II. FACTORIZATION: FORMULATION AND APPLICATION

Our approach to strong decays is similar in spirit to what was done decades past for electromagnetic and current induced transitions among hadrons, known variously as Melosh transformation or more generally “single quark transition algebra”[10]. The empirically successful hypothesis there was that the interaction of a current with a single quark triggers a transition, all other constituents being passive spectators. That led to algebraic relations among amplitudes, which arose from the clebsch-gordan coefficients coupling the orbital, spin and total angular momentum projections l_z, s_z to j_z for the initial and final hadrons, and the l_z, s_z algebraic transformation properties of the transition operators. While the relative strengths of the reduced matrix elements associated with each transition operator are in this general approach undetermined, the experimentally accessible range of helicity amplitudes for photo-excitation of proton and neutron targets to different resonances within a supermultiplet led to experimentally testable relations among various amplitudes[11]. Within the hypothesis of l, s factorization, analogous relations arise for strong decays. Specific models have implicitly assumed such factorization[5, 6, 12, 13, 14]; we shall see that the results from lattice QCD suggest that this property is realised in decays at least for light flavours.

We consider the decay process of mesons $M \rightarrow M_1 + M_2$. In meson M with spin j , the $q\bar{q}$ have spin s and residual angular momentum l . We illustrate the structure of the amplitude for the particular case of a flux-tube that breaks to form a new $q\bar{q}$ in a 3P_0 configuration leading to a pair of mesons M_1, M_2 with spins j_1, j_2 respectively, and their $q\bar{q}$ having s_1, l_1, s_2, l_2 . The generalisation will be immediate.

The width for the decay of a meson into a pair of mesons involves a sum over couplings of $j_1 \otimes j_2$ to j_{12} and relative partial waves L :

$$\Gamma(slj \rightarrow s_1 l_1 j_1 + s_2 l_2 j_2) \sim \sum_{j_{12} L} \langle (((s_1 \otimes l_1)_{j_1} \otimes (s_2 \otimes l_2)_{j_2})_{j_{12}} \otimes L)_j | |\sigma \cdot \nabla| | (s \otimes l)_j \rangle^2 \quad (2)$$

where σ transforms as a vector in spin-space and ∇ acts on the spatial (orbital and radial) degrees of freedom. Usually at this point specific wavefunctions are assumed and nonrelativistic expressions calculated for the amplitudes[5, 6, 12, 13, 14]. However, this introduces model dependence and obscures the more general underlying properties. Instead we shall factor the amplitude in such a way that the spin and space parts are separated [15], expressing all decay amplitudes as linear combinations of model-dependent spatial amplitudes, which in the present work are left general.

The first step is to separate the spin and space degrees of freedom of the final state. The final state bra

$$\langle (((s_1 \otimes l_1)_{j_1} \otimes (s_2 \otimes l_2)_{j_2})_{j_{12}} \otimes L)_j | \quad (3)$$

is recoupled to form states of good (s_{12}, l_{12}, l_f) :

$$\langle ((s_1 \otimes s_2)_{s_{12}} \otimes ((l_1 \otimes l_2)_{l_{12}} \otimes L)_{l_f})_j | \quad (4)$$

which involves a product of 6- j and 9- j coefficients. The spin and space parts then factorise and can be isolated. The result is

$$\begin{aligned} \langle (((s_1 \otimes l_1)_{j_1} \otimes (s_2 \otimes l_2)_{j_2})_{j_{12}} \otimes L)_j | |\sigma \cdot \nabla| | (s \otimes l)_j \rangle &= \sum_{s_{12} l_{12} l_f} (-)^{s+L+s_{12}+l_{12}+l_f} \Pi_{l_f s_{12} l_{12} j_1 j_2 j_{12}} \\ &\left\{ \begin{matrix} s_1 & l_1 & j_1 \\ s_2 & l_2 & j_2 \\ s_{12} & l_{12} & j_{12} \end{matrix} \right\} \left\{ \begin{matrix} s_{12} & l_{12} & j_{12} \\ L & j & l_f \end{matrix} \right\} \left\{ \begin{matrix} s_{12} & s & 1 \\ l & l_f & j \end{matrix} \right\} \langle (s_1 \otimes s_2)_{s_{12}} | |\sigma| | s \rangle \langle ((l_1 \otimes l_2)_{l_{12}} \otimes L)_{l_f} | |\nabla| | l \rangle \end{aligned} \quad (5)$$

with

$$\Pi_{ab\dots} = \sqrt{(2a+1)(2b+1)\dots} \quad (6)$$

The spin part is a 9- j coefficient along with appropriate counting factors

$$\langle (s_1 \otimes s_2)_{s_{12}} | |\sigma| | s \rangle = (-)^{s+s_1} \Pi_{1 s s_1 s_2 s_{12}} \left\{ \begin{matrix} \frac{1}{2} & \frac{1}{2} & s_1 \\ \frac{1}{2} & \frac{1}{2} & s_2 \\ s & 1 & s_{12} \end{matrix} \right\}. \quad (7)$$

The $9-j$ coefficient in eqn. (7) is zero for $s_1 = s_2 = s = 0$; this is the well known spin singlet selection rule and is a consequence of the orthogonality of the spin wavefunctions. Note in the above a phase of (-1) has been included for the permutation of quark and antiquark operators [9], and the expression (5) is equivalent to that in Ref. [16].

The assumption driving the expansion of eqn. (5) is that the angular momentum and spin quantum numbers factorize and that the decay operator is overall scalar with a spin triplet part. The angular momentum algebra makes no reference to the spatial part of the operator, hence the linear combinations for 3P_0 and 3S_1 decay models, driven by operators $\sigma \cdot \nabla$ and $\sigma \cdot \hat{\mathbf{r}}$ respectively, are the same. In a 3S_1 model the spatial contraction involves $\hat{\mathbf{r}}$ - the unit vector in the relative coordinate of the initial meson's $q\bar{q}$. In specific models this has a different spatial dependence but the overall spin coupling coefficients are identical.

Eqn. (5) expresses full decay amplitudes $a_{j_{12}L}$ as linear combinations of model dependent spatial amplitudes $A_{l_{12}Ll_f}$ of the form

$$A_{l_{12}Ll_f} = \langle ((l_1 \otimes l_2)_{l_{12}} \otimes L)_{l_f} || \nabla || l \rangle \quad (8)$$

These spatial amplitudes are momentum dependent and depend on radial wavefunctions. The angular momentum algebra thus relates decay amplitudes among families of states sharing the same spatial quantum numbers but having different spin and total angular momentum, in the limit that the spatial wavefunctions of the mesons under comparison are the same and the momenta are the same. If for a given partial wave L there is only one spatial matrix element of the form (8), which we denote A_L , there are direct relations among amplitudes for states with different angular momentum quantum numbers. Three such cases are immediate:

1. one of the final states has orbital angular momentum zero ($l_2 = 0$) and the decay is in relative S -wave ($L = 0$); thus $l_f = l_{12} = l_1$ and the amplitude is expressed in terms of a single matrix element A_S ;
2. both final states have orbital angular momentum zero ($l_1 = l_2 = 0$); thus $l_{12} = 0$ and $l_f = L$ and the amplitude in a partial wave L can be expressed in terms of a single matrix element A_L ;
3. the initial state and one of the final states have orbital angular momentum zero ($l = l_2 = 0$), thus $l_{12} = l_1$ and $l_f = 1$ and the amplitude in a partial wave L can be expressed in terms of a single matrix element A_L .

We now examine each of these three cases in turn with specific examples. In section II A the S -wave hybrid decays $\pi_1 \rightarrow b_1\pi$ and $\pi_1 \rightarrow f_1\pi$ are shown to match results from lattice QCD and thereby to reveal significant information about the underlying dynamics (case 1). In section II B, $a_1 \rightarrow \rho\pi$ and $b_1 \rightarrow \omega\pi$ are examples of case 2; the analysis verifies a conjecture that was made elsewhere [9] and establishes its origin. In section II C case 3 is applied to derive relations among decays of the type ${}^3S_1 \rightarrow ({}^1P_1; {}^3P_j) + ({}^1S_0; {}^3S_1)$. A new selection rule is derived and the possibility of testing it in the context of e^+e^- annihilation producing flavoured and flavourless states is discussed. In section II D we discuss ways of using these results to distinguish hybrid $c\bar{c}$ from 3S_1 or 3D_1 ψ states.

A. S -wave decays of hybrid meson π_1

An immediate example of this factorization is the S -wave decays of the hybrid meson $\pi_1 \rightarrow b_1\pi$ or $f_1\pi$. The π_1 has 1^{-+} quantum numbers and $j = s = l = 1$ [5, 6]. The final states have $l_1 = j_1 = 1$ and $s_2 = l_2 = j_2 = 0$, differing in the spin quantum number $s_1 = 0$ (b_1) and $s_1 = 1$ (f_1). For decays in S -wave there is only one matrix element of the form (8), having $l_{12} = l_f = 1$. In the summation over l_{12} and l_f , this constraint is enforced by zeroes in the 9 - and $6-j$ coefficients which reduce to delta functions. This reduces the expansion of eqn. (5) to a simpler form and the amplitude for the initial state with spin s_1 is given by

$$a_S({}^3P_1 \rightarrow^{s_1} P_1 + {}^1S_0) = \frac{3}{\sqrt{2}} \Pi_{s_1} \left\{ \begin{matrix} s_1 & 1 & 1 \\ 1 & 1 & 1 \end{matrix} \right\} \left\{ \begin{matrix} 1/2 & 1/2 & s_1 \\ 1 & 1 & 1/2 \end{matrix} \right\} \times A_S \quad (9)$$

where here A_S is the spatial matrix element. Thus for the 1P_1 and 3P_1 modes

$$a_S({}^3P_1 \rightarrow {}^1P_1 {}^1S_0) = -\frac{A_S}{2\sqrt{3}} \quad (10)$$

$$a_S({}^3P_1 \rightarrow {}^3P_1 {}^1S_0) = -\frac{A_S}{2\sqrt{6}} \quad (11)$$

The flavour overlaps for $\pi_1 \rightarrow b_1\pi$ and $f_1(n\bar{n})\pi$ are $\sqrt{2/3}$ and $\sqrt{1/3}$, so that the ratio of amplitudes is

$$\frac{a_S(\pi_1 \rightarrow b_1\pi)}{a_S(\pi_1 \rightarrow f_1\pi)} = 2 \quad (12)$$

which underwrites the result eq.(1) as found also in lattice QCD. The essential feature here is the factorization of spin and space, and the assumption that the created $q\bar{q}$ are spin-triplet. Note that the $q\bar{q}$ creation with quark-spin 1 now appears explicitly in 9- j and 6- j symbols. To see the sensitivity here, contrast with the possibility that the created pair been spin-singlet: in this case the final 9- j symbol for the πb_1 mode, equation (7), has a zero in the bottom left corner, and since

$$\left\{ \begin{array}{ccc} \frac{1}{2} & \frac{1}{2} & 0 \\ \frac{1}{2} & \frac{1}{2} & 0 \\ 0 & 1 & 0 \end{array} \right\} = 0 \quad (13)$$

the decay $\pi_1 \rightarrow \pi + b_1(^1P_1)$ would vanish. More directly this can be understood since if spin is conserved, an initial state with $S = 1$ can only decay to a pair of $S = 0$ states if $S = 1$ $q\bar{q}$ is present, hence the need for pair-creation to be spin-triplet for a non-zero amplitude.

Thus the results of lattice QCD, at least when applied to the decays of a hybrid meson[7], follow if the amplitude factors in space and spin, with the $q\bar{q}$ pair creation being spin-triplet and an overall scalar. This does not distinguish 3P_0 from 3S_1 decay models.

B. S and D wave decays of axial mesons

Ackleh et al[9] noted that the ratio of the D/S -wave amplitudes for $b_1 \rightarrow \omega\pi$ and $a_1 \rightarrow \rho\pi$ can be a sensitive discriminator among models. They found that if the $q\bar{q}$ are created in the 3P_0 configuration, as commonly assumed in flux-tube models, the ratio of D/S ratios is

$$\frac{\frac{a_D}{a_S}(a_1 \rightarrow \rho\pi)}{\frac{a_D}{a_S}(b_1 \rightarrow \omega\pi)} = -\frac{1}{2}. \quad (14)$$

They found the same ratio in the case of $q\bar{q}$ creation by gluon exchange in the static limit (“colour coulomb”) but that it departs from $-1/2$ in the case of transverse gluon exchange. It was suggested that this might be useful as a signature of the one-gluon exchange component in the physical decay amplitude, and noted that experimentally the ratio is -0.35 ± 0.09 [9], 2σ away from $-1/2$. Today the ratio

$$\frac{\frac{a_D}{a_S}(a_1 \rightarrow \rho\pi)}{\frac{a_D}{a_S}(b_1 \rightarrow \omega\pi)} = -0.39 \pm 0.06 \quad (15)$$

has a greater precision[17] due to recent experiments[18], though the statistical deviation from $-1/2$ remains similar. Although the authors of ref [9] speculated that the common ratio for 3P_0 and coulomb-gluon cases is because of a lack of spin-flip, which is violated in the case of transverse gluon exchange and hence the deviation from $-1/2$ in that case, they did not explicitly demonstrate the source.

In the factorisation scheme, the amplitude for these decays is proportional to a single matrix element; this is an example of case 2 cited above. Once again, zeroes in the Wigner coefficients reduce the expansion of eqn. (5) to a simpler form and enforce the conservation of angular momentum ($l_{12} = 0$ and $l_f = L$), whereby the amplitude in a partial wave L is proportional to a unique spatial matrix element A_L . The two decay modes of interest differ in the spin quantum number of the initial state, $s = 0$ (b_1) and $s = 1$ (a_1). The amplitudes are given by

$$a_L(^sP_1 \rightarrow ^3S_1 \ ^1S_0) = \frac{3}{\sqrt{2}}(-)^{L+s_1}\Pi_s \left\{ \begin{array}{ccc} 1 & s & 1 \\ 1 & L & 1 \end{array} \right\} \left\{ \begin{array}{ccc} 1/2 & 1/2 & 1 \\ 1 & s & 1/2 \end{array} \right\} \times A_L \quad (16)$$

This gives

$$a_S(^1P_1 \rightarrow ^3S_1 \ ^1S_0) = -\frac{1}{2\sqrt{3}}A_S \quad a_D(^1P_1 \rightarrow ^3S_1 \ ^1S_0) = -\frac{1}{2\sqrt{3}}A_D \quad (17)$$

$$a_S(^3P_1 \rightarrow ^3S_1 \ ^1S_0) = -\frac{1}{\sqrt{6}}A_S \quad a_D(^3P_1 \rightarrow ^3S_1 \ ^1S_0) = \frac{1}{2\sqrt{6}}A_D \quad (18)$$

Thus we have established that the ratio eqn. (14) is an immediate result of the factorization and $q\bar{q}$ creation with spin 1. A deviation from this ratio is indicative of a breaking of factorization, such as by a transverse gluon which transfers spin and momentum (“spin-orbit coupling”) in general. We shall return to this mechanism for breaking of factorization in section III.

C. S and D wave decays of vector mesons

matrix element A_S, A_D ; this is an example of case 3 discussed earlier. Decays of vector mesons provide a range of tests of factorization and decay dynamics. Decays of the type

$$^3S_1 \rightarrow ^3P_{0,1,2} + ^3S_1 \quad (19)$$

$$^3S_1 \rightarrow ^3P_{1,2} + ^1S_0 \quad (20)$$

$$^3S_1 \rightarrow ^1P_1 + ^3S_1 \quad (21)$$

$$^3S_1 \rightarrow ^1P_1 + ^1S_0 \quad (22)$$

all belong to the special case 3 described earlier; their decay amplitudes in a partial wave L are each proportional to a unique matrix element A_L . Substituting into eqn. (5) $l = 0, s = j = 1$ for the initial state and $l_1 = 1$ and $l_2 = 0$ for the final states gives the amplitude $a_{j_{12}L}$ for the decay in a partial wave L with final states coupled to j_{12} :

$$a_{j_{12},L}(^3S_1 \rightarrow ^{s_1}P_{j_1} + ^{s_2}) = \sum_{s_{12}} (-)^{L+j_1+1} \Pi_{1s_1s_2s_{12}s_{12}j_1j_{12}} \begin{Bmatrix} s_1 & s_{12} & s_2 \\ j_{12} & j_1 & 1 \end{Bmatrix} \begin{Bmatrix} s_{12} & 1 & j_{12} \\ L & 1 & 1 \end{Bmatrix} \begin{Bmatrix} \frac{1}{2} & \frac{1}{2} & s_1 \\ \frac{1}{2} & \frac{1}{2} & s_2 \\ 1 & 1 & s_{12} \end{Bmatrix} \times A_L \quad (23)$$

The results are shown in Table I below. The pattern of amplitudes is realized in specific model calculations that have implicitly assumed factorization, e.g.[13], which give explicit expressions for the spatial dependences $A_{S(n)}$ and $A_{D(n)}$ for radial excitations n . The amplitudes in Table I differ from those in Ref. [13] by a phase associated with the ordering of the angular momentum couplings.

$^3S_1 \rightarrow ^3P_0 \ ^3S_1$	$a_{1S} = -A_S/2$ $a_{1D} = 0$
$^3S_1 \rightarrow ^3P_1 \ ^3S_1$	$a_{1S} = A_S/\sqrt{3}$ $a_{1D} = A_D/4\sqrt{3}$ $a_{2D} = A_D/4$
$^3S_1 \rightarrow ^3P_2 \ ^3S_1$	$a_{1S} = 0$ $a_{1D} = A_D/4\sqrt{5}$ $a_{2D} = -A_D/4\sqrt{3}$ $a_{3D} = -A_D\sqrt{7/15}$ $a_{3G} = 0$
$^3S_1 \rightarrow ^1P_1 \ ^3S_1$	$a_{1S} = A_S/\sqrt{6}$ $a_{1D} = -A_D/2\sqrt{6}$ $a_{2D} = -A_D/2\sqrt{2}$
$^3S_1 \rightarrow ^1P_1 \ ^1S_0$	$a_{1S} = A_S/2\sqrt{3}$ $a_{1D} = A_D/2\sqrt{3}$
$^3S_1 \rightarrow ^3P_1 \ ^1S_0$	$a_{1S} = A_S/\sqrt{6}$
$^3S_1 \rightarrow ^3P_1 \ ^1S_0$	$a_{1D} = -A_S/2\sqrt{6}$
$^3S_1 \rightarrow ^3P_2 \ ^1S_0$	$a_{2D} = A_D/2\sqrt{2}$

TABLE I: Decay amplitudes $a_{j_{12}L}$ for the decays (19)-(22)

1. $\psi(n^3S_1) \rightarrow$ **flavoured mesons**

The results of Table I can be applied immediately to $\psi(n^3S_1) \rightarrow D_{0,2}D^*$ and also to $D_1D^{(*)}$. In the latter case data may be used to determine the mixing angle between 1P_1 and 3P_1 .

The eigenstates for axial flavoured mesons are in general mixtures of the 3P_1 and 1P_1 states. Ref.[19] defines the mixing angles by

$$\begin{aligned} |D_{1L}\rangle &= \cos\phi |^1P_1\rangle + \sin\phi |^3P_1\rangle \\ |D_{1H}\rangle &= -\sin\phi |^1P_1\rangle + \cos\phi |^3P_1\rangle \end{aligned} \quad (24)$$

and discusses ways of determining them experimentally. The amplitudes for axial meson production as a function of mixing angle follow from Table I with careful treatment of phase conventions for the spin-mixed states. For $q\bar{c}$ states (as opposed to $c\bar{q}$ states) and with orbital and spin angular momentum combined in the order $(l \otimes s)_j$, the heavy quark limit gives $\phi = -54.7^\circ$ [20] so that the states are

$$\begin{aligned} |\bar{D}_{1L}\rangle &= \sqrt{\frac{1}{3}}|{}^1P_1\rangle - \sqrt{\frac{2}{3}}|{}^3P_1\rangle \\ |\bar{D}_{1H}\rangle &= \sqrt{\frac{2}{3}}|{}^1P_1\rangle + \sqrt{\frac{1}{3}}|{}^3P_1\rangle \end{aligned} \quad (25)$$

The amplitudes of eqn. (5), shown in Table I, are for the topology in which the created q (\bar{q}) ends up in the meson with quantum numbers $s_1 l_1 j_1$ ($s_2 l_2 j_2$). If the axial states are labelled with the quantum numbers $s_1 l_1 j_1$ they are $q\bar{c}$ states in accordance with conventions of ref [20]. On the other hand, our amplitudes apply to meson spin coupling in the order $(s \otimes l)_j$ so there is relative minus sign associated with the 3P_1 part of the amplitude. Thus for the mixed $\bar{D}_{1H}, \bar{D}_{1L}$ states in the heavy quark limit, the amplitudes for ${}^3S_1 \rightarrow \bar{D}_{1L}D, \bar{D}_{1H}D$ are

$$a_{j_{12}L}({}^3S_1 \rightarrow \bar{D}_{1L}D) = \sqrt{\frac{1}{3}}a_{j_{12}L}({}^3S_1 \rightarrow {}^1P_1 {}^1S_0) + \sqrt{\frac{2}{3}}a_{j_{12}L}({}^3S_1 \rightarrow {}^3P_1 {}^1S_0), \quad (26)$$

$$a_{j_{12}L}({}^3S_1 \rightarrow \bar{D}_{1H}D) = \sqrt{\frac{2}{3}}a_{j_{12}L}({}^3S_1 \rightarrow {}^1P_1 {}^1S_0) - \sqrt{\frac{1}{3}}a_{j_{12}L}({}^3S_1 \rightarrow {}^3P_1 {}^1S_0), \quad (27)$$

and likewise for ${}^3S_1 \rightarrow \bar{D}_{1L}D^*, \bar{D}_{1H}D^*$. This gives the relative decay widths (up to phase space corrections) shown in Table II below.

	S^2	D^2
$D_0 D^*$	1	0
$D_{1L} D^*$	2	0
$D_{1H} D^*$	0	1
$D_2 D^*$	0	2
$D_{1L} D$	1	0
$D_{1H} D$	0	$\frac{1}{2}$
$D_2 D$	0	$\frac{1}{2}$

TABLE II: Relative widths ${}^3S_1 \rightarrow D^* D_{0,1,2}$ or $DD_{0,1,2}$; the states $D_{1L,H}$ are light and heavy axial mesons in the heavy quark limit.

Hence in the heavy quark limit

$$\Gamma(\psi(n^3S_1) \rightarrow D^* D_{1L}) = 2\Gamma(\psi(n^3S_1) \rightarrow DD_{1L}) \quad (28)$$

$$\Gamma(\psi(n^3S_1) \rightarrow D^* D_{1H}) = 2\Gamma(\psi(n^3S_1) \rightarrow DD_{1H}) \quad (29)$$

as well as

$$\Gamma(\psi(n^3S_1) \rightarrow D^* D_{1L}) = 2\Gamma(\psi(n^3S_1) \rightarrow D^* D_0) \quad (30)$$

$$\Gamma(\psi(n^3S_1) \rightarrow D^* D_{1H}) = \frac{1}{2}\Gamma(\psi(n^3S_1) \rightarrow D^* D_2) \quad (31)$$

$$\Gamma(\psi(n^3S_1) \rightarrow DD_{1H}) = \Gamma(\psi(n^3S_1) \rightarrow DD_2) \quad (32)$$

In addition there is a selection rule that the D_2 is produced only in helicity 0 or 1; *i.e* denoting helicity states by $0, (\pm), (\pm\pm)$ then

$$a(\psi(n^3S_1) \rightarrow \bar{D}_2(\pm\pm)D^*(\mp)) = 0 \quad (33)$$

This will be derived in the next section.

2. Helicity selection rule

In the factorization scheme, the decay of a transversely polarised ${}^3S_1 \rightarrow {}^3P_2 + {}^3S_1$, with the tensor meson maximally polarised along the decay axis, is predicted to vanish:

$$a({}^3S_1(+) \rightarrow {}^3P_2(++) {}^3S_1(-)) = 0 \quad (34)$$

This selection rule is a test of factorization; a significant non-zero strength for this helicity amplitude in a decay $1^{--} \rightarrow 1^{--} 2^{++}$ signals either a breakdown of factorization or the presence of 3D_1 in 1^{--} or of 3F_2 in 2^{++} . The origin of the selection rule is most transparent if we consider the helicity amplitude structure directly. Its generality can then be assessed by transforming to partial wave amplitudes.

First consider the helicity picture. The decay is

$$q_1 \bar{q}_4 \rightarrow [q_1 \bar{q}_2] + [q_3 \bar{q}_4] \quad (35)$$

through the creation of $\bar{q}_2 q_3$ (Fig 1). Denoting fermions with $S_z = \pm 1/2$ by u, d respectively, the initial ${}^3S_1(+)$ has its $q\bar{q}$ spins oriented $u_1 u_4$. The final ${}^3P_2(++) {}^3S_1(-)$ then has to be $[u_1 \bar{u}_2] + [d_3 \bar{d}_4]$ (or $[12]$ interchanged with $[34]$) with the $[u_1 \bar{u}_2]$ also having $L_z = +1$. For either configuration, spin-flip is required for a non-vanishing amplitude.

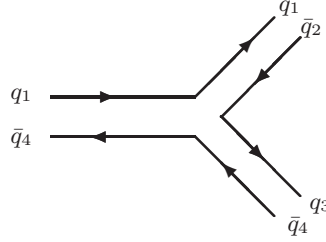


FIG. 1: Strong decay topology.

Spin conservation on spectator lines following the steps above, or the diagrammatic techniques of ref. [9], enable relations among helicity amplitudes to be calculated in such factorizing models.

In order to expose the more general dynamics underpinning this selection rule, and to exhibit the relations among the various helicity amplitudes, it is useful to transform between helicity and partial wave amplitudes. As before, consider a state with spin j decaying to two particles with spins respectively j_1, j_2 . The final state can be characterised by quantum numbers (j_{12}, L) or by helicity quantum numbers (λ_1, λ_2) ; the translation between the two bases, for an initial state with spin projection m along some axis, is given by

$$|jm; \lambda_1, \lambda_2\rangle = \sum_{Lj_{12}} \sqrt{\frac{2L+1}{2j+1}} \langle j_{12}\lambda | j_1\lambda_1; j_2-\lambda_2 \rangle \langle j\lambda | j_{12}\lambda; L0 \rangle |jm; j_{12}L\rangle \quad (36)$$

This enables helicity amplitudes $a_{\lambda_1\lambda_2}$ to be written as linear combinations of partial wave amplitudes $a_{j_{12}L}$. We are interested here in decays of the type

$$V(\lambda) \rightarrow \chi_{j_1}(\lambda_1) + V(-\lambda_2) \quad (37)$$

with $\lambda_1 - \lambda_2 = \lambda$, the relation between helicity and partial wave amplitudes follows from (36) above with $j = j_2 = 1$,

$$a_{\lambda_1\lambda_2} = \sqrt{\frac{1}{3}} \langle 1\lambda | j_1\lambda_1; 1-\lambda_2 \rangle a_{1S} + \sqrt{\frac{5}{3}} \sum_{j_{12}} \langle 1\lambda | j_{12}\lambda; 20 \rangle \langle j_{12}\lambda | j_1\lambda_1; 1-\lambda_2 \rangle a_{j_{12}D} + \sqrt{3} \langle 1\lambda | 3\lambda; 40 \rangle \langle 3\lambda | j_1\lambda_1; 1-\lambda_2 \rangle a_{3G} \quad (38)$$

The resulting relations are shown in the first column of Table III. These relations apply generically to the decay of any vector meson to any scalar, axial or tensor meson χ_{j_1} . For decays of the type

$${}^3S_1(\lambda) \rightarrow {}^3P_{j_1}(\lambda_1) + {}^3S_1(-\lambda_2), \quad (39)$$

where each of the vectors are explicitly in a 3S_1 state and the χ_{j_1} is a ${}^3P_{j_1}$ state, the amplitude follows substituting for $a_{j_{12}L}({}^3S_1 \rightarrow {}^3P_{j_1} {}^3S_1)$ from Table I; the results are shown in the second column of Table III. The selection rule (34) is explicit in the last line of Table III and follows immediately substituting

$$a_{1S} = a_{3G} = 0; \quad a_{1D} = A_D/4\sqrt{5}; \quad a_{2D} = -A_D/4\sqrt{3}; \quad a_{3D} = -A_D\sqrt{7/15}; \quad (40)$$

	$V(\lambda) \rightarrow \chi_{j_1}(\lambda_1) + V(-\lambda_2)$	${}^3S_1(\lambda) \rightarrow {}^3P_{j_1}(\lambda_1) + {}^3S_1(-\lambda_2)$
$j_1 = 0$	$a_{0,0} = a_{1S}/\sqrt{3} - a_{1D}/\sqrt{2/3}$	$= -A_S/2\sqrt{3}$
	$a_{0,+} = a_{1S}/\sqrt{3} + a_{1D}/\sqrt{6}$	$= -A_S/2\sqrt{3}$
$j_1 = 1$	$a_{0,0} = 0$	$= 0$
	$a_{+,0} = a_{1S}/\sqrt{6} + a_{1D}/\sqrt{12} - a_{2D}/2$	$= A_S/3\sqrt{2} - A_D/12$
	$a_{0,+} = -a_{1S}/\sqrt{6} - a_{1D}/\sqrt{12} - a_{2D}/2$	$= -A_S/3\sqrt{2} - A_D/6$
	$a_{+,-} = a_{1S}/\sqrt{6} - a_{1D}/\sqrt{3}$	$= A_S/3\sqrt{2} - A_D/12$
$j_1 = 2$	$a_{0,0} = -a_{1S}\sqrt{2/15} + 2a_{1D}/\sqrt{15} + 3a_{3D}/\sqrt{35} - 2a_{3G}\sqrt{3/35}$	$= -A_D/2\sqrt{3}$
	$a_{+,0} = -a_{1S}/\sqrt{10} - a_{1D}/\sqrt{20} - a_{2D}/\sqrt{12} + 4a_{3D}/\sqrt{105} + 2a_{3G}/\sqrt{35}$	$= -A_D/4$
	$a_{0,+} = a_{1S}/\sqrt{30} + a_{1D}/\sqrt{60} + a_{2D}/2 + 2a_{3D}/\sqrt{35} + a_{3G}\sqrt{3/35}$	$= -A_D/2\sqrt{3}$
	$a_{+,-} = a_{1S}/\sqrt{10} - a_{1D}/\sqrt{5} + a_{3D}\sqrt{3/35} - 2a_{3G}/\sqrt{35}$	$= -A_D/4$
	$a_{++,-} = a_{1S}/\sqrt{5} + a_{1D}/\sqrt{10} - a_{2D}/\sqrt{6} + a_{3D}\sqrt{2/105} + a_{3G}/\sqrt{70}$	$= 0$

TABLE III: Column 1 expresses helicity amplitudes $a_{\lambda_1\lambda_2}$ in terms of partial wave amplitudes $a_{j_{12}L}$ for decays (37) of generic vector states. Column 2 expresses helicity amplitudes in terms of spatial amplitudes A_L for decays (39) with explicit s and l quantum numbers.

In general the selection rule requires that the partial-waves a_{1S} and $a_{3G} \equiv 0$ and that the $a_{j_{12}D}$ conspire. The amplitude $a_{3G} \equiv 0$ in 3P_0 or 3S_1 models since $(l_{12} = l_2 = 1) \otimes (L = 3)$ can couple to $(l_f = 2, 3, 4)$, which cannot couple to the $l = 0$ initial state by the vector decay operators ∇ or $\hat{\mathbf{r}}$. The appearance of this zero can be tested by measurement of the various helicity amplitudes which satisfy the linear relation

$$a_{0,0} - 2/\sqrt{3}a_{+,0} + 2/\sqrt{3}a_{+,-} = a_{0,+} + 1/\sqrt{6}a_{++,-} \quad (41)$$

The selection rule $V(+) \rightarrow T(++)V(-) = 0$ can be violated by failure of factorization, such as when single gluon exchange produces the \bar{q}_2q_3 and flips-spin such as $u_1 \rightarrow d_1$, or if there are 3D_1 admixtures in the wavefunctions of the produced or initiating vector mesons. The general property that breaks factorization and mixes 3D_1 components in the produced vector meson is essentially the same: in models the latter is generated by spin-orbit coupling, such as from gluon exchange[21]. To the extent that vector mesons and e^+e^- annihilation are dominated by 3S_1 configurations, and the strong decay amplitude factorizes, the selection rule will apply. For the $\psi(4415)$, which is consistent with being 4^3S_1 [26], the decays $\psi(4415) \rightarrow DD_2$ have been observed by ISR [23]; our selection rule may be testable on the high mass side of the $\psi(4415)$ in its decays to the low mass tails of $D^*(2010)$ and $D_2(2460)$ respectively. It can also be tested in the e^+e^- continuum immediately around 4.5GeV as 3D_1 contamination is expected to be minimal[26].

D. Hybrid and Exotic Charmonium

While 3S_1 ψ states are expected to dominate the couplings to e^+e^- annihilation, there are local $c\bar{c}$ resonance structures in in the 4-5GeV energy range whose structure is still unestablished[26]. In particular there are the enigmatic structures $Y(4260)$ and $Y(4325)$ [24]. These have no natural assignment within $c\bar{c}$ spectroscopy and explanations include hybrid charmonium, or molecules (e.g. by either $cq\bar{c}\bar{q}$ tetraquarks or DD_1 and D^*D_0 attractive forces via π exchange), or even effects associated with S-wave charmed meson thresholds[25].

These states are near to the S-wave thresholds for $DD_1, D^*D_{0,1,2}$. Such decays are an example of case 1 discussed earlier: each S-wave amplitude is proportional to a single spatial matrix element. The coefficient is a function of the spin and orbital angular momentum of the vector initial state, and thus the pattern among decay amplitudes differs for ${}^3S_1, {}^3D_1$ and hybrid interpretations, where for the latter the $c\bar{c}$ have $l = 1$ and $s = 0$. Eqn. (5) gives the coefficient of the spatial matrix element, and the results are shown in Table IV. For axial mesons the amplitudes are shown in both the 1P_1 - 3P_1 basis and in heavy quark limit, where for the latter the amplitudes are given by eqns. (26) and (27) and their analogues.

If production of charmed mesons in the decays of 3S_1 $c\bar{c}$ is confirmed to factorise, then using Table IV the relative decay amplitudes to $DD_1, D^*D_{0,1,2}$ may be used to determine the structure of $c\bar{c}$ states that are near to the S-wave thresholds. In particular this applies to $Y(4260)$ and $Y(4325)$. There are characteristic zeroes that may occur for

	3S_1	3D_1	$^1\Pi P_1$
$D_0 D^*$	$-1/2$	0	$1/3\sqrt{2}$
$D_1(^1P_1)D^*$	$1/\sqrt{6}$	$-1/2\sqrt{6}$	$1/2\sqrt{3}$
$D_1(^3P_1)D^*$	$1/\sqrt{3}$	$1/4\sqrt{3}$	$1/2\sqrt{6}$
$D_2 D^*$	0	$1/4\sqrt{5}$	$-\frac{1}{6}\sqrt{\frac{5}{2}}$
$D_1(^1P_1)D$	$1/2\sqrt{3}$	$1/2\sqrt{3}$	0
$D_1(^3P_1)D$	$1/\sqrt{6}$	$-1/2\sqrt{6}$	$-1/2\sqrt{3}$
$D_{1L}D$	$1/2$	0	$-1/3\sqrt{2}$
$D_{1H}D$	0	$1/2\sqrt{2}$	$1/6$

TABLE IV: Relative S wave amplitudes for vector charmonia decays with 3S_1 , 3D_1 and $^1\Pi P_1$ (hybrid) configurations; the states D_{1L} , D_{1H} refer to axial mesons in the heavy quark limit.

vector meson decays:

$$\Gamma(^3S_1 \rightarrow D_{1H}D) = 0 \quad (42)$$

$$\Gamma(^3D_1 \rightarrow D_{1L}D) = 0 \quad (43)$$

$$\Gamma(^1\Pi P_1(\text{hybrid}) \rightarrow D_1(^1P_1)D) = 0 \quad (44)$$

The first pair of zeroes arise from the affinity of light and heavy D_{1L} , D_{1H} for S and D couplings respectively, and the zero (42) was noted by ref. [26]. For the hybrid decay the result follows from the conclusion of lattice QCD, section IIA, that decays are driven by $q\bar{q}$ creation in spin-triplet, which implies that a pair of spin-singlets (such as D and 1P_1) cannot be produced from a spin-singlet, such as a hybrid vector $c\bar{c}$. In practice these predictions will be affected by mixing, which can be determined from other processes (e.g. see [19]), and by phase space. The relative rates are insensitive to form factor effects at low momenta (see for example refs [12, 13, 19]).

III. ELECTRON-POSITRON ANNIHILATION

For e^+e^- annihilation at a fixed $q^2 \equiv E_{c.m.}^2$, if one models the decay as occurring via the intermediary of virtual radially-excited vector 3S_1 $Q\bar{Q}$ states, the relative amplitudes to pairs of $q\bar{q}$ mesons in either of 1S_0 , 3S_1 together with 1P_1 , 3P_j will have the pattern of Table I for each and every radial excitation, n . So long as there is not an unfortunate double conspiracy where both a single n dominates and also a node in its amplitude coincides with the kinematic region of interest, the amplitudes of Table I may be generalized to e^+e^- annihilation. This may be checked by varying q^2 to see if the ratios are stable or vary in an oscillatory or nodal manner. The assumption that $e^+e^- \rightarrow Q\bar{Q}$ is dominated by 3S_1 is reasonable above charm threshold where the coupling $e^+e^- \rightarrow ^3D_1(c\bar{c})$ is theoretically and empirically suppressed[17, 26]. The results of Table I then apply immediately to $e^+e^- \rightarrow D^*D_{0,2}$ and also to $D^{(*)}D_1$, which in the latter case may be used to determine the mixing angle between 1P_1 and 3P_1 . While this is strictly true on a 3S_1 ψ resonance, it may also be expected to hold through the 4-5 GeV region of interest where 3S_1 is predicted to dominate the e^+e^- cross section.

Application to $e^+e^- \rightarrow \psi + \chi_j$ also follows if this is dominated by strong flux-tube formation and breaking. We shall argue in section IIIB that this is more likely to be dominated by (perturbative) gluon exchange, which breaks factorization and gives a different pattern of amplitudes than strong flux-tube breaking. Our results may be used to test this hypothesis.

In the case of light flavours the neglect of $e^+e^- \rightarrow ^3D_1(q\bar{q})$ is more questionable. The leptonic widths of $^3D_1(q\bar{q})$ are nonetheless expected to be relatively small[27], and empirically the known vector mesons appear to fit well with (radially excited) 3S_1 with some mixing with hybrid vectors without need for significant 3D_1 [28]. This is clearly an area whose phenomenology merits further clarification. To that end we apply our results with 3S_1 dominance to light flavours in the hope of shedding further light on this sector and isolating 3D_1 states. For ψ decays this simple assumption appears to be consistent with existing data[17, 29].

A. $e^+e^- \rightarrow$ flavourless mesons

In the case of $e^+e^- \rightarrow$ neutral states, charge conjugation restricts the production of axial-vector mesons in association with 0^{-+} or 1^{-+} to $e^+e^- \rightarrow V + ^3P_1$ or $^1S_0 + ^1P_1$. The amplitudes of Table I apply and the relative rates then follow

by application of equation (5):

$$^3S_1 + ^3P_0 : ^3S_1 + ^3P_1 : ^3S_1 + ^3P_2 : ^1S_0 + ^1P_1 = 3S^2 : 4S^2 + D^2 : 6D^2 : S^2 + D^2 \quad (45)$$

and hence

$$\sigma(^3S_1 + ^3P_1) = \frac{4}{3}\sigma(^3S_1 + ^3P_0) + \frac{1}{6}\sigma(^3S_1 + ^3P_2) \quad (46)$$

together with

$$3\sigma(^1S_0 + ^1P_1) = \sigma(^3S_1 + ^3P_0) + \frac{1}{2}\sigma(^3S_1 + ^3P_2) \quad (47)$$

and their corollary

$$\sigma(^1S_0 + ^1P_1) = \frac{1}{8}\sigma(^3S_1 + ^3P_2) + \frac{1}{4}\sigma(^3S_1 + ^3P_1). \quad (48)$$

Note that necessarily

$$\sigma(e^+e^- \rightarrow ^3S_1 + ^3P_1) > \sigma(e^+e^- \rightarrow ^3S_1 + ^3P_0). \quad (49)$$

For flavoured states the two axial mesons are mixtures of 1P_1 and 3P_1 ; whatever the mixing angle may be, the inequality holds true in the sense that the $^3S_1 + ^3P_0$ production rate cannot exceed those of both of axial mesons. In the case of charge conjugation eigenstates we are restricted to applying it to light flavours or to $e^+e^- \rightarrow \psi + \chi_j$. The former case is less well controlled theoretically, due to relativistic effects and potential contamination from 3D_1 background in e^+e^- annihilation, though the above relations appear to be consistent with data and are discussed in ref.[29]. One of the central applications of the present paper will be to test these predictions against data on $e^+e^- \rightarrow \psi + \chi_j$ where preliminary indications are that the relation eq.(49) is violated[30]. This is discussed in section IIIB.

The amplitude $V(-)T(++)$, where here T denotes a tensor meson, should also be measured for light flavours where VT modes are prominent, especially in ψ decay. Within the factorization hypothesis and 3S_1 dominance the Vf_2 cannot be produced with f_2 maximally polarised; $a[e^+e^- \rightarrow V(j_z = -1)f_2(j_z = +2)] = 0$. This may be studied in $e^+e^- \rightarrow 5\pi = 2\pi^+2\pi^-\pi^0$ by isolating the channel ωf_2 ; the ω being a narrow state can enable the angular distribution in decay $f_2 \rightarrow \pi^+\pi^-$ to be measured. The main background here is the potential contamination from e^+e^- annihilation in the 3D_1 state. Although models and data do not suggest this is significant, nonetheless one cannot rule it out. If the amplitude is empirically found to be small, in accord with the selection rule, one could turn this to advantage and study the amplitude as a function of q^2 in the hope of finding it turning on and off as one passed through predicted 3D_1 resonances around 2.2GeV[27].

B. Factorization breakdown and preformation by OgE

Data on $e^+e^- \rightarrow \psi + X$ at 10.6 GeV c.m. energy show three prominent enhancements X in $e^+e^- \rightarrow \psi + X$ [30], which are consistent with being the η_c, η'_c and χ_0 . The observed pattern of states appears radically different to what is seen for light flavours, for example the apparent prominence of $e^+e^- \rightarrow \psi + \chi_0$ with only a hint of χ_1 and much suppressed χ_2 contrasts with light flavours where $e^+e^- \rightarrow \omega f_2$ is clearly seen[17]. This suggests that this process for heavy flavours may be controlled by a production mechanism where factorization is broken.

On theoretical grounds one expects that strong factorization may be overwritten here. In e^+e^- annihilation at $E > 6$ GeV, creation of an initial $c\bar{c}$ leaves up to 3 GeV available. As the $c\bar{c}$ separate, forming a strong flux tube up to $O(1fm)$ long, the energy of $O(1GeV)$ enables light-flavoured $q\bar{q}$ to form. That is the familiar dynamics that appears to be realized at low energies for light flavours. In the present example, the most probable circumstance is that the excess energy produces multiple $q\bar{q}$ leading to final states $D\bar{D}\pi\pi\dots$. The experimental selection on final states $\psi X(c\bar{c})$ isolates an unlikely configuration where the 3 GeV has produced a $c\bar{c}$ exclusively. For the flux tube to grow without splitting until it contains 3 GeV of energy would require it to extend to distances exceeding Λ_{QCD}^{-1} . This is exponentially unlikely with increasing energy.

Alternatively the energy can be transmitted through a single gluon which converts to $c\bar{c}$. While this is perturbative and expected to be sub-dominant for processes involving light flavour creation, the question arises at what energy or

for what flavours this dominates over flux-tube breaking. The purpose of this section is to propose ways of answering this by experiment. We make specific reference to $e^+e^- \rightarrow (c\bar{c}) + (c\bar{c})$ as there are emerging data in the form of $e^+e^- \rightarrow \psi + X$.

As momentum flows through the gluon, it can transfer spin or angular momentum between the $c\bar{c}$ to which it is coupled. In general therefore we anticipate that factorization will break down.

Ref [9] have considered these matrix elements in the explicit non-relativistic limit - (see Appendix B of ref [9], especially eqs B5-B7). In that limit the gluon-exchange operation transforms as **S.S** and **L.S** but there is no **S.L** operator (where the first operator refers to the transformation property of the gluon emission and the second operator to that of $q\bar{q}$ creation). Thus in the strict non-relativistic limit of that model, the $V(-)T(++)$ selection rule would appear to survive for the decay of a 3S_1 vector meson. This is no surprise following the discussion after eq.(34) : non-zero amplitude requires spin flip at the emission vertex and orbital flip at the $c\bar{c}$ creation vertex; while the former occurs in the non-relativistic limit, the latter does not.

However, in e^+e^- annihilation at $q^2 \equiv E_{c,m}^2$, the production of a $c\bar{c}$ allows an **S.L** operator at $O(q^2/m_c^2)$. An explicit calculation of the gluon exchange contributions to $e^+e^- \rightarrow \psi + \chi_j$ has been made in NRQCD in ref [31] and a non-vanishing amplitude for $V(-)T(++)$ is found even at threshold, in accord with the discussion above. Threshold is when $q^2 = 16m_c^2$; the amplitudes depend upon $r^2 \equiv 16m_c^2/q^2$. At high energies, where $r^2 \rightarrow 0$ the contribution from $e^+e^- \rightarrow ^3D_1 \rightarrow c\bar{c}$ will become increasingly important while for the threshold region, $r^2 \rightarrow 1$, the $e^+e^- \rightarrow ^3S_1 \rightarrow c\bar{c}$ becomes more dominant.

At the 10.6 GeV c.m. energy of the data [30], $r^2 = 0.28$, and ref [31] finds for the OgE contribution to the cross sections $\sigma(\psi\chi_0 : \psi\chi_1 : \psi\chi_2) \sim 12 : 2 : 3$, which contradicts eq.(49) based upon factorization and assumption of a 3S_1 initial state. In the threshold limit $r^2 \rightarrow 1$ the analysis simplifies and comparison between the predictions of gluon exchange and factorization becomes sharpest. In this limit the VT amplitudes for transversely polarised initial state of ref.[31] satisfy

$$a[V(-)T(++)] : a[V(0)T(+)] : a[V(+)T(0)] = 1 : 1/\sqrt{2} : 1/\sqrt{6} \quad (50)$$

in accord with S-wave dominance and the results of Table III. The relative cross-sections from the single gluon exchange mechanism (OgE) for $e^+e^- \rightarrow \psi\chi_{0,1,2}$ in vicinity of threshold $r^2 \rightarrow 1$ in ref [31] become

$$\sigma(\psi\chi_0 : \psi\chi_1 : \psi\chi_2) \sim 24 : 2 : 3. \quad (51)$$

Compared to the results at higher energy, $r^2 = 0.28$, the relative sizes of $\psi\chi_1 : \psi\chi_2$ have not changed much but there is a significant relative enhancement of $\sigma(\psi\chi_0)$ near threshold.

This prediction, that the cross-section for $\psi\chi_0$ dominates, contrasts with the results of factorization near threshold. For 3S_1 initial state in the S -wave region near threshold

$$\begin{aligned} \sigma(\psi\chi_2) &\rightarrow 0 \\ \sigma(\psi\chi_0) &= \frac{3}{4}\sigma(\psi\chi_1) \end{aligned} \quad (52)$$

Analogously, for a 3D_1 initial state

$$\begin{aligned} \sigma(\psi\chi_0) &\rightarrow 0 \\ \sigma(\psi\chi_1) &= \frac{5}{3}\sigma(\psi\chi_2) \end{aligned} \quad (53)$$

which is also utterly unlike the OgE predictions. Finally one may allow for a coherent mixture of 3S_1 and 3D_1 initial state. Results become model dependent but $\sigma(\psi\chi_0)$ cannot be made larger than both $\sigma(\psi\chi_1)$ and $\sigma(\psi\chi_2)$. Thus in the region of threshold there appear to be marked differences in the expectations of factorization, eqs (52),(53) and OgE eq.(51).

As one increases energy above threshold, for 3S_1 initial state, the D -wave decay enables $\sigma(\psi\chi_2)$ to turn on but with the amplitude $a[V(-)T(++)] = 0$ or at least small compared to $a[V(0)T(+)]$ and $a[V(+)T(0)]$. This also contrasts with the predictions from OgE where the $[V(-)T(++)]$ amplitude is the largest for VT production, eq(50). A possible contamination comes from $e^+e^- \rightarrow ^3D_1 \rightarrow c\bar{c}$ contributions which may not be negligible at 6-7GeV c.o.m energies. The S-wave decay amplitudes from initial $^3S_1, ^3D_1$ and also from hybrid vector mesons are compared in Table IV. Above threshold where D -wave decays are important and 3S_1 - 3D_1 mixing is allowed, results are highly

model dependent. While it may be possible to force $\sigma(\psi\chi_0)$ to dominate by suitable choice of mixing angle, this is not expected to hold true as a function of q^2 .

Thus if dominance of $\psi\chi_0$ is confirmed over a range of q^2 away from threshold, this would support OgE as the dominant decay mechanism. Conversely, if data near threshold confirm $a[V(-)T(++)] \rightarrow 0$, this would signal factorization being dominant. In any event, we anticipate that the relative populations and helicity structures of $\psi\chi_j$ will vary with q^2 . We recommend that this be investigated in e^+e^- annihilation at super-B factories by means of ISR to access a range of energies. In particular experiment should attempt to measure the spin dependence of $e^+e^- \rightarrow \psi\chi_2$ as a function of q^2 and compare with the analogous amplitudes in $e^+e^- \rightarrow \omega f_2$.

IV. CONCLUSION

The factorization property of strong decay triggered by $q\bar{q}$ creation in spin-triplet, as revealed by lattice QCD, merits further testing. These general features lead to relations among amplitudes, which can be used as further tests of this dynamics and to determine the nature of participating mesons. Thus we have identified the following tests.

1. $\psi(n^3S_1)$ decays or e^+e^- annihilation in the 4-5 GeV energy range will not produce D^*D_2 with the tensor meson in helicity two. This tests whether the dynamics revealed by lattice QCD for light mesons applies more generally for the strong creation of light flavours.
2. If confirmed, then the production $e^+e^- \rightarrow D^{(*)}D_1$ may be used to determine the axial meson mixing angles in the 3P_1 - 1P_1 bases.
3. If the mixing angles are known from elsewhere, the pattern of charm pair production can identify the nature of the decaying ψ state. This has an application of immediate relevance in determining the nature of the enigmatic charmonium-like structures $Y(4260)$ and $Y(4325)$ and also of $\psi(4415)$. Determining whether the $c\bar{c}$ content of these states is $S = 0$ (as for a hybrid) or $S = 1$ then follows from the relative production rates of various combinations of charmed mesons, in particular of their DD_1 branching ratios.
4. The application to light flavours in e^+e^- is less solid, but measurement of the ωf_2 amplitudes as a function of q^2 may isolate 3D_1 resonances in the e^+e^- channel.
5. For the creation of heavy flavours, as in $e^+e^- \rightarrow \psi\chi_j$, empirical and theoretical arguments suggest that production is dominated by a single hard gluon rather than the factorization mechanism. The apparent excess of $\psi\chi_0$ and absence of $\psi\chi_2$ needs establishing. We expect that the pattern of χ_j states and their helicity amplitudes will vary significantly with q^2 . We identify the threshold region $e^+e^- \rightarrow \psi\chi_j$ between 6.5 and 7.5 GeV as particularly promising for determining the relative importance of single hard gluon and strong factorization for heavy flavours.

We are grateful to E.Swanson for discussions. This work is supported, in part, by grants from the Science and Technology Facilities Council, the Oxford University Clarendon Fund and the EU-TMR program ‘Eurodice’, HPRN-CT-2002-00311.

-
- [1] G Bali *et al*, (UKQCD Collaboration), Phys. Lett. B309 378 (1993);
C Morningstar and M J Peardon, Phys. Rev. D60 034509 (1999)
 - [2] P Lacock, C Michael, P Boyle and P Rowland, Phys. Lett. B401 308 (1997)
 - [3] N Isgur and J Paton, Phys. Rev. D **31** 2910 (1985).
 - [4] T Barnes, F E Close, and E S Swanson, Phys. Rev. D **52** 5242 (1995).
 - [5] N Isgur, R Kokoski and J Paton, Phys. Rev. Lett. **54** 869 (1985).
 - [6] F E Close, and P R Page, Nucl. Phys. B **443** 233 (1995).
 - [7] C Michael and C McNeile, arXiv:hep-lat/0603007; Phys.Rev. D73 074506 (2006)
 - [8] T J Burns and F E Close, Phys.Rev. D74 034003 (2006)
 - [9] E Ackleh, T Barnes and E Swanson, arXiv:hep-ph/9604355; Phys.Rev. D54 6811 (1996)

- [10] H J Melosh, Phys. Rev. D9 1095 (1974)
 A J G Hey and J Weyers, Physics Letters 48B 69 (1974)
 F E Close and F J Gilman, Physics Letters 38B 541 (1972)
 F E Close, H Osborn and A M Thomson, Nucl. Phys. B77 281 (1974)
 F E Close *Introduction to Quarks and Partons* (Academic Press 1979), Chap 7
- [11] V Burkert and T Lee, Chap 3 in *Electromagnetic Interactions and Hadronic Structure* (eds. F E Close, A Donnachie and G Shaw), Cambridge University Press (2007)
- [12] A Le Yaouanc, L Oliver, O Pene and J Raynal, Phys. Rev. D8 2223 (1973); G Busetto and L Oliver, Z. Phys. C20 247 (1983); R Kokoski and N Isgur, Phys. Rev. D35 907 (1987); P Geiger and E Swanson, Phys. Rev. D50 6855 (1994); H G Blundell and S Godfrey, Phys. Rev. D53 3700 (1996)
- [13] T Barnes, F E Close, P R Page and E Swanson, Phys. Rev. D55 4157 (1997)
- [14] P R Page, E S Swanson, and A P Szczepaniak, Phys. Rev. D **59**, 034016 (1999)
- [15] T J Burns, arXiv:hep-ph/0611132
- [16] R Bonnaz and B Silvestre-Brac, Few Body Systems 27 (1999) 163
- [17] Particle Data Group, J Phys G 33 1 (2006)
- [18] M Nozar *et al* (MPS Collaboration), Physics Letters **B541**, 35 (2002)
 S Chung *et al* (E852 Collaboration), Phys. Rev. **D65** 072001 (2002)
- [19] F E Close and E S Swanson, arXiv:hep-ph/0505206; Phys. Rev. **D72** 094004 (2005)
- [20] E S Swanson, arXiv:hep-ph/0601110; Phys. Rept. **429** 243 (2006)
- [21] N Isgur and G Karl, Phys. Rev. D23 817 (1981)
- [22] T Barnes, S Godfrey and E Swanson, arXiv:hep-ph/0505002; Phys Rev D72, 054026 (2005);
 T Barnes, arXiv:hep-ph/0406327
- [23] G Pakhlova *et al*, (BELLE Collaboration), arXiv:0708.3313
- [24] B Aubert *et al* (BaBar Collaboration), arXiv:hep-ex/0506081; Phys.Rev.Lett. 95 (2005) 142001
 B Aubert *et al* (BaBar Collaboration), arXiv:hep-ex/0610057; Phys. Rev. Lett. 98, 212001 (2007).
- [25] F E Close, *Rumsfeld Hadrons*, arXiv 0706.2709; Proceedings of FPCP07 (2007).
- [26] T Barnes, S Godfrey and E Swanson, arXiv:hep-ph/0505002, Phys. Rev. D72, 054026 (2005)
- [27] S Godfrey and N Isgur, Phys Rev D32, 189 (1985).
- [28] F E Close, A Donnachie and Y Kalashnikova, in *Electromagnetic Interactions and Hadronic Structure* (CUP 2007); Chap 4.
- [29] T Burns and F E Close *Hadronic Decays of Charmonium* (in preparation)
- [30] Belle Collaboration, K Abe *et al.*, arXiv:hep-ex/0507019, BaBar Collaboration, B Aubert *et al*, arXiv:hep-ex/0506062.
- [31] E Braaten and J Lee, arXiv:hep-ph/0211085; Phys.Rev. D67 (2003) 054007; Erratum-ibid. D72 099901 (2005)